Electronic Supplementary Material (ESI) for Physical Chemistry Chemical Physics

Efficient cyanoaromatic photosensitizers for singlet oxygen production: synthesis and characterization of the transient reactive species

Filippo Ronzani,[a] Emmanuel Arzoumanian,[b] Sylvie Blanc,[a] Patrice Bordat,[a] Thierry Pigot,[a] Cyril Cugnet,[a] Esther Oliveros,[b] Mohamed Sarakha,[c] Claire Richard,[c] Sylvie Lacombe*[a]

Section SI 1

Synthesis of compounds 3 and 4.

Synthesis of 3-(N-hydroxypropyl)carboxamido-9,14-dicyanobenzo[b]triphenylene (DBTP-CO-NH-$(CH_2)_3$-OH, **3**). **2** (185 mg, 1 eq) was dissolved at 35°C in 65 mL of freshly distilled THF. The system was let under stirring at room temperature for 1 hour. Then DCC (152 mg, 1.2 eq) and NHS (102 mg, 1.2 eq) were added. The basicity of the reaction mixture was assured by adding 100 μL of Et_3N. The reaction mixture was let under stirring for 4 hours, until complete conversion took place. 3-amino-1-propanol (1.2 mL, 2 eq) was added directly into the flask. The reaction, which was followed by thin layer chromatography, was let running for 24 hours. After evaporating the solvent, the product was dissolved in methylene chloride and washed successively with 5% $NaHCO_3$ solution, 5% citric acid solution and brine. The organic fraction was dried over $MgSO_4$ during the night and purified by preparative thin layer chromatography, yielding compound **3** as a yellow powder in 40% yield.

mp 273 °C. Elemental analysis not available due to the presence of traces of *N*,*N'*-cyclohexylurea. IR (KBr): ν_{max} /cm^{-1} 625m (N-H bending), 752s and 839w (C-H bending), 1057br (C-O stretching, alcohol), 1437m (C-N stretching, amide), 1497m and 1541s (N-H bending, amide, and C=C stretching, aromatics), 1647s (C=O stretching), 2200s (CN stretching), 2864br and 2943br (C-H stretching), 3066br (C-H stretching, aromatics), 3384br (NH and OH stretching). ^{1}H NMR δ_H (Figure SI 2, ESI) (400.13 MHz, DMSO-d_6; Me_4Si): 9.33 and 9.30 (1H+1H, 2d, J=8.5 Hz, J=8.1 Hz, CH_1 and CH_8), 9.16 (1H, s, CH_4), 8.88 (1H, d, J=8.1 Hz, CH_5), 8.57 (2H, m, CH_{11+12}), 8.21 (1H, d, J=8.5 Hz, CH_2), 8.12 (2H, m, CH_{10+13}), 7.96 and 7.86 (1H+1H, 2t, J=8.1 Hz CH_6 and CH_7), 8.97 (1H, m, NH), 4.57 (1H, m, OH). ^{13}C NMR not available due to the low solubility of the product. MS (ESI): m/z 430.15533 ($C_{28}H_{20}O_2N_3$, MH^+), 355.08661 ($C_{25}H_{11}ON_2^+$, MH^+ - HO-$(CH_2)_3$-NH_2), 327.09109 ($C_{24}H_{11}N_2$, MH^+- HO-$(CH_2)_3$-NH_2-CO). (HPLC-UV chromatogram in Fig.SI 5, ESI).

Synthesis of 3-(N-N'-Boc-aminohexyl)carboxamido-9,14-dicyanobenzo[b]triphenylene (DBTP-CO-NH-$(CH_2)_6$-NH-Boc, **4**). **2** (250 mg, 1 eq) was dissolved in 200 mL of dried chloroform. After 1 hour stirring at room temperature NHS (100 mg, 2 eq) and EDC (150 mL, 2 eq) were added under N_2 flow at 0°C. After 24 hours *N*-Boc-1,6-hexanediamine (150 mL, 1.6 eq) was added. The reaction was let running for 24 hours, then the solvent was evaporated and the crude product was purified by column chromatography, yielding a yellow powder in 65% yield.

mp 175-178 °C. Elemental analysis (%) for $C_{36}H_{34}N_4O_3$, calculated C 75.8, H 6.0, N 9.8, O 8.4; found C 74.0, H 6.0, N 9.6, O 8.7. IR (KBr): ν_{max} /cm^{-1} 623m (N-H bending), 750s and 841w (C-H bending),

1174s (C-O stretching, carbamate), 1363m (CH_3 bending), 1448w (C-N stretching, amide and carbamate), 1497s and 1535m (N-H bending, amide and carbamate, and C=C stretching, aromatics), 1658s (C=O stretching, amide), 1707s (C=O stretching, carbamate), 2200s (CN stretching), 2858m, 2929br and 2974m (C-H stretching), 3060w (C-H stretching, aromatics), 3386s (NH stretching). ^{1}H NMR δ_H (400.13 MHz, $CDCl_3$; Me_4Si, Fig.SI 3, ESI): 9.26 (1H+1H, t, J=9 Hz, CH_1 and CH_8), 8.98 (1H, s, CH_4), 8.55 (1H+2H, m, CH_5 and CH_{11+12}), 7.95 (1H, d, J=8 Hz, CH_2), 7.86 (2H, m, CH_{10+13}), 7.71 and 7.64 (1H+1H, 2t, J=7 Hz, J=9 Hz, CH_6 and CH_7), 6.88 (1H, s, NH-amide), 4.62 (1H, m, NH-carbamate), 3.50 (2H, dt, J=7 Hz, CH_2NH-amide), 3.12 (2H, m, CH_2-NH-carbamate), 1.66 (2H, m, *CH_2*CH_2NH-amide), 1.54 and 1.46 (6H, 3m, *$CH_2CH_2CH_2$*CH_2NH-carbamate), 1.35 (9H, s, t-butyl). ^{13}C NMR (100.61 MHz, $CDCl_3$, Fig.SI 4, ESI): 166.5 (CONH), 156.3 (OCONH, Boc), 136.1 (CCONH), 133.6, 132.3, 132, 130.3, 128.7, 127.8, 125.5, 125.2, 124.1, 123.4 (CH), 132.6, 131.6, 130.8, 130.2, 128.3, 127.7, 126.8, 126.3 (C quat.), 118.2 (CN), 108.5, 108.1 (CCN), 79.2 (C quat., Boc), 39.9, 39.7 (CH_2NH), 30.3, 30.2, 29.4, 26.0 (CH_2), 28.5 (CH_3, *t*-butyl). MS (ESI): m/z = 571.21793 ($C_{36}H_{35}O_3N_4$, MH^+), 515.20752 (MH^+ - C_4H_8), 471.21793 MH^+ - $OCOC_4H_8$), 355.08627 ($C_{25}H_{11}ON_2^+$). (HPLC-UV chromatogram in Fig.SI 6, ESI).

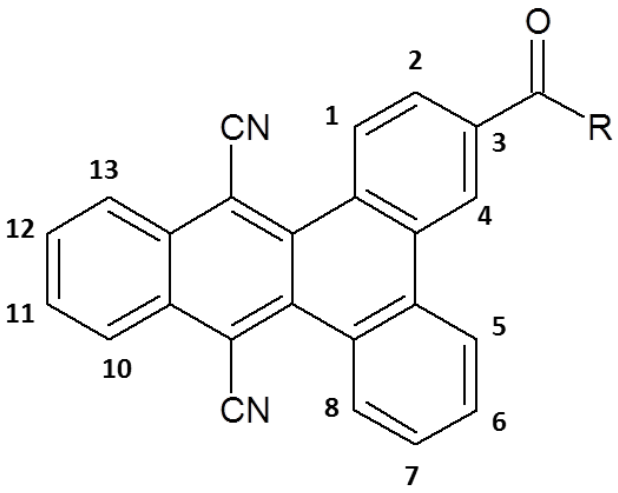

Figure SI 1 Chart with atom numbering for compounds **2**, **3** and **4**.

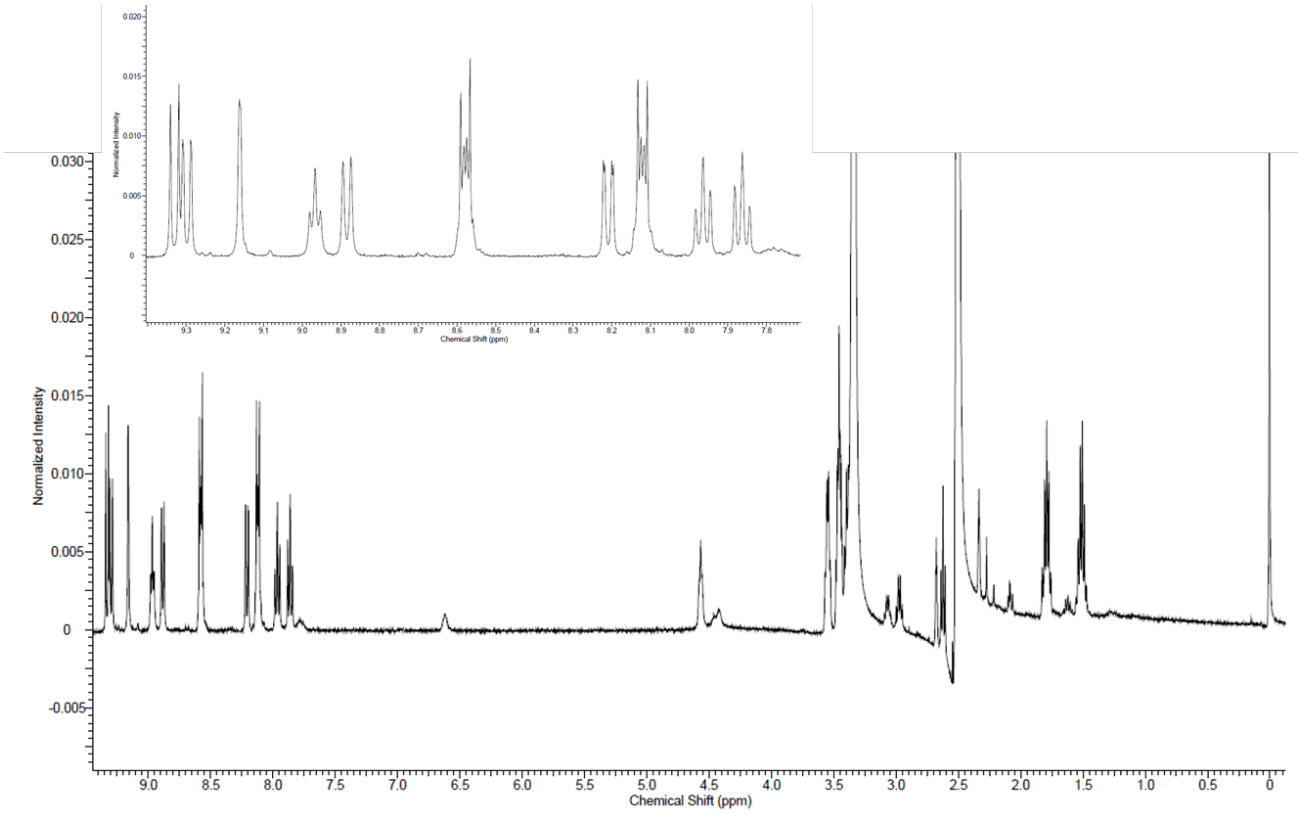

Figure SI 2 ^{1}H NMR spectrum of **3**. Inset: detailed aromatic peaks.

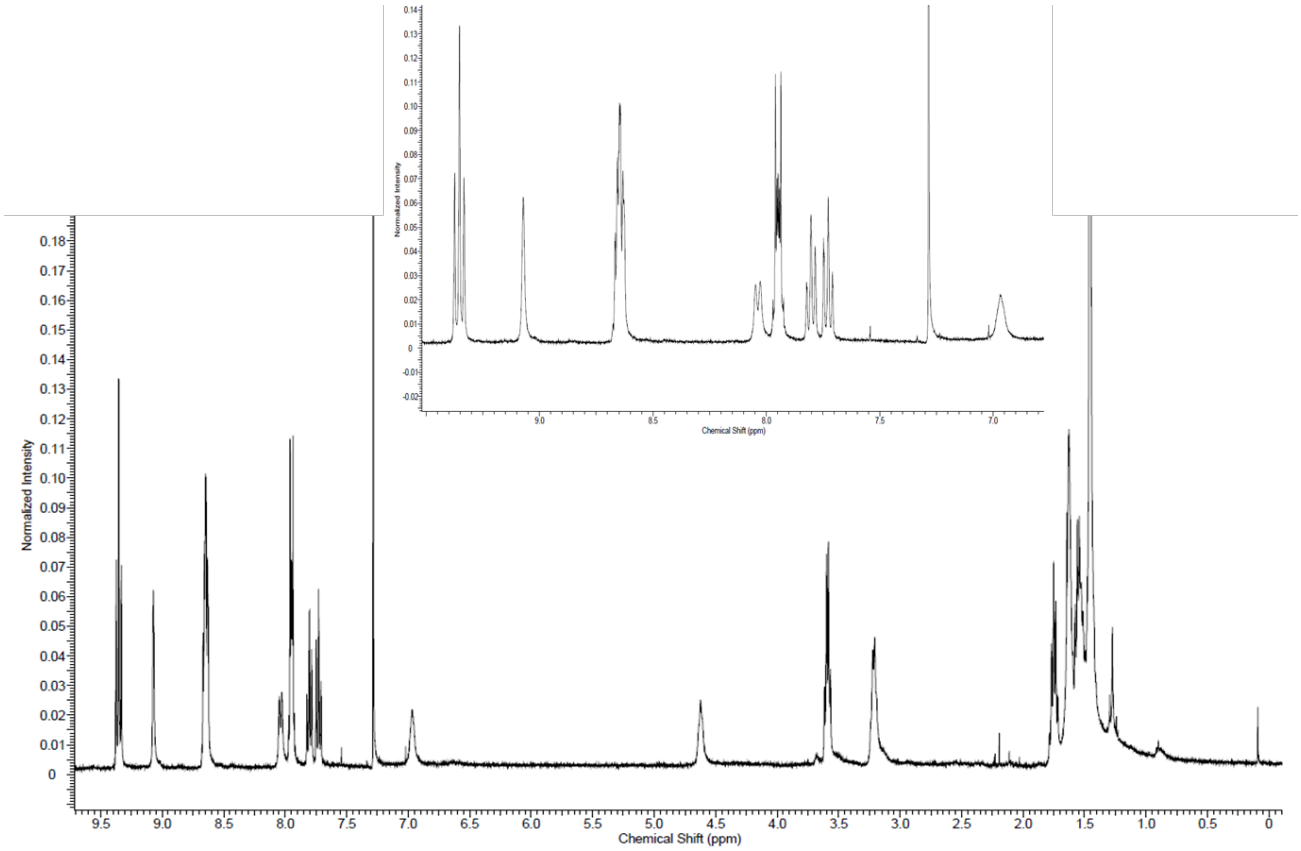

Figure SI 3 ^{1}H NMR spectrum of **4**. Inset: detailed aromatic peaks. Chemical shifts were corrected taking into account the slight shift of TMS relative to 0 ppm.

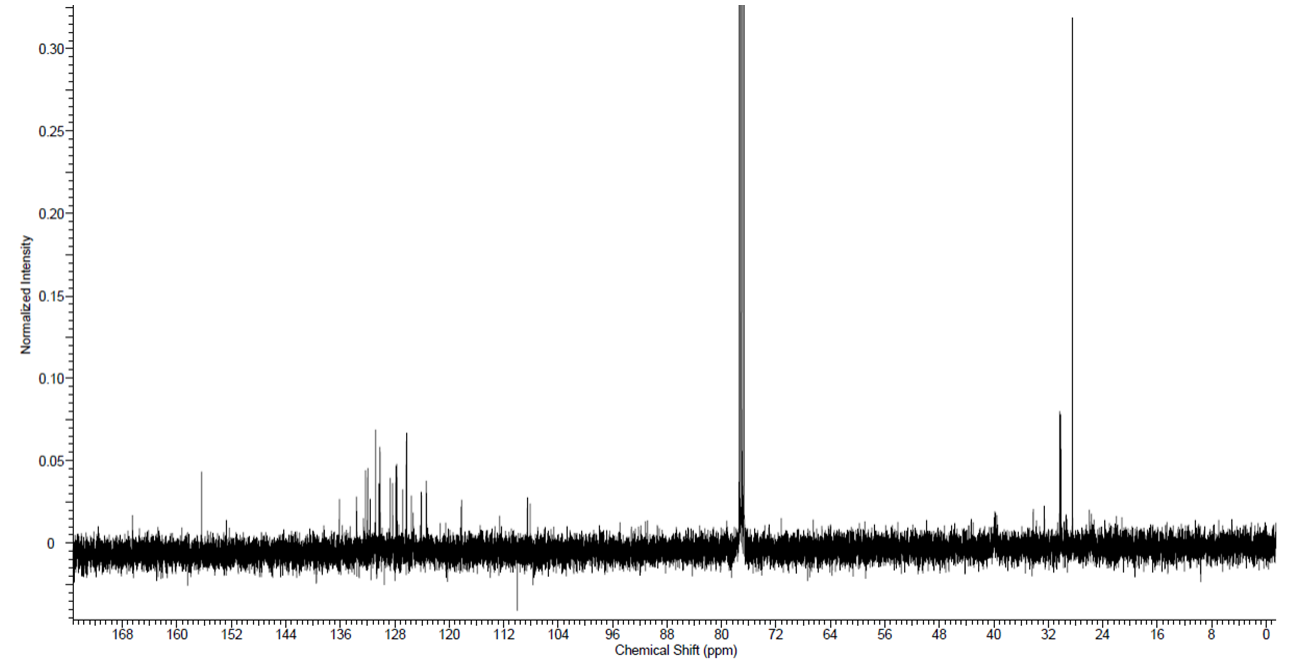

Figure SI 4 ^{13}C NMR spectrum of **4**.

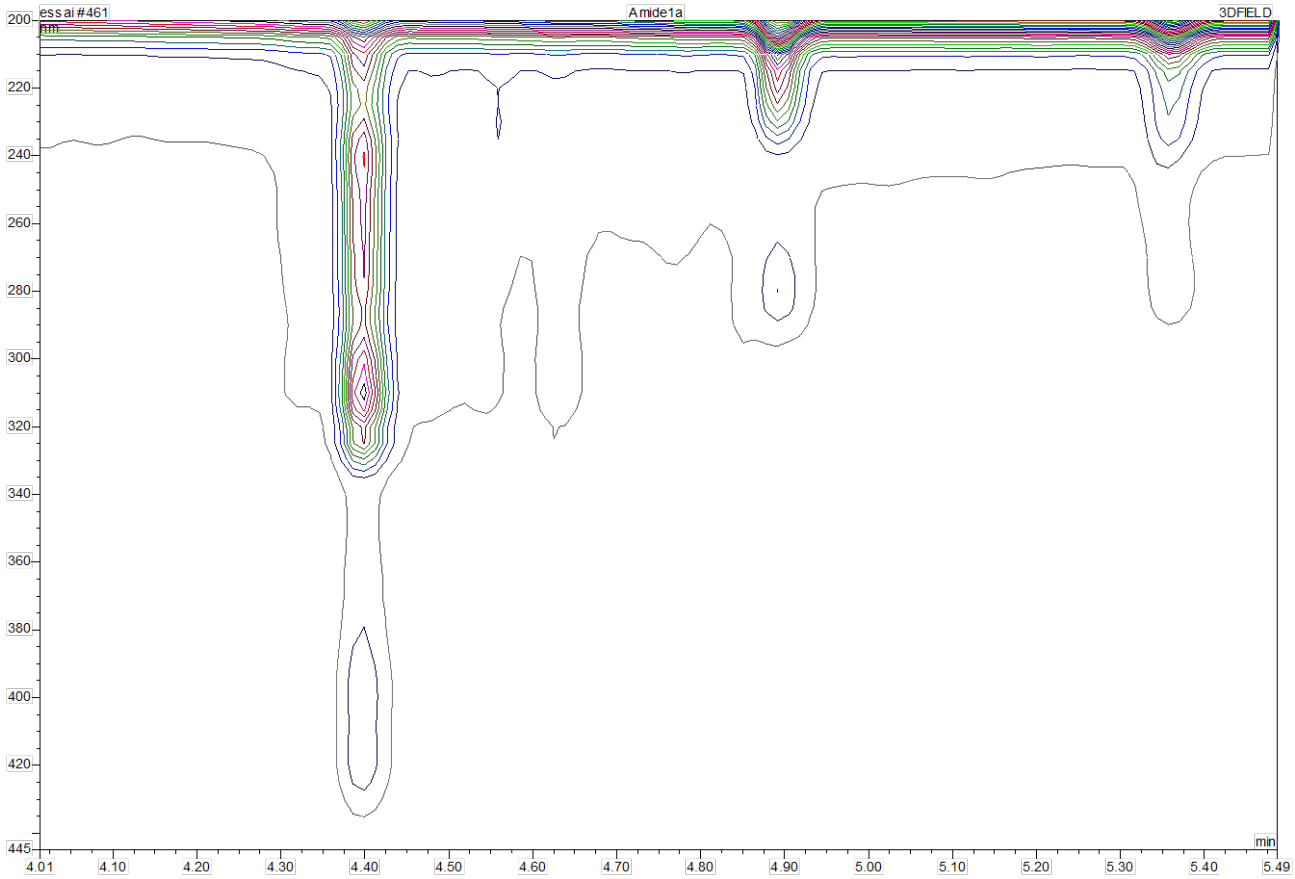

Figure SI 5 HPLC chromatogram of **3**.

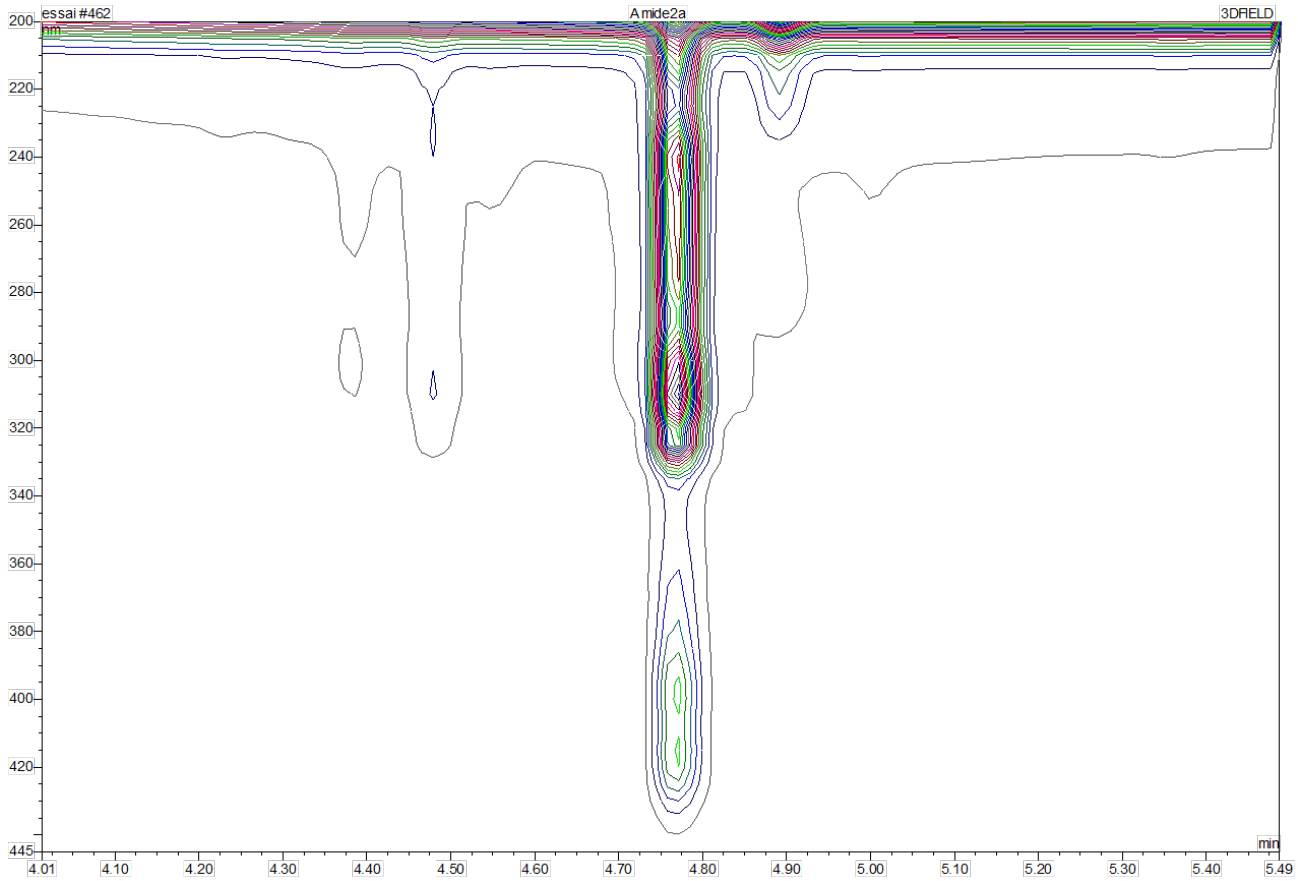

Figure SI 6 HPLC chromatogram of **4**.

Section SI 2

Operating conditions for NMR, MS and cyclic voltammetry.

A standard pulse sequence (90° pulse and relaxation delay of 5 s) was used for ^{1}H NMR spectra. The spectral width and size of time domain data set were 8250 Hz and 64 K respectively. Exponential multiplication with a line broadening factor of 0.3 Hz was employed throughout.

MS spectra were registered under the following conditions: Ion transfer 350°C, Vaporizer 300°C, Sheath gas 35°C, Auxiliary gas 10°C, Spray voltage 3kV. The resolution in mass was 60 000 at m/z 400. The spectra were recorded between m/z 100 and 600 and the spectrometer was calibrated just before measurements for a mass precision <1.5-2 ppm. The products were introduced through an UHPLC-U3000 (Dionex) with a BEH (Waters) column (50 x 2.1 I.D. mm, particle size 1.8 µm) at a flow rate of 0.25 mL min^{-1} using a linear gradient from 10 % A and 90% B to 95 % A and 5 % B in 5 minutes, where A=water + 0.1% formic acid and B= acetonitrile + 0.1 % formic acid.

All electrochemical experiments were performed in 60 mL of acetonitrile containing 0.1 M of tetrabutylammonium bromide as supporting electrolyte. Solutions were degassed with N_2 before use. The molecules were characterized by rotating disk electrode voltammetry with a potential range from -0.5 to -1.3 V at scan rates 50 mV s^{-1}.

The procedure for TDDFT optimization of the structure of **DCA** and **1** at the DFT level was carried out with the B3LYP functional and the 6-31G* basis using Gaussian09 package.[1] This optimization has been carried out in vacuum as well as in heptane and ethanol using the PCM model.[2] From the optimized structures, Time-Dependent Density Functional Theory (TDDFT) calculations have been performed at the B3LYP/6-31G* level in vacuum and in PCM model of heptane and ethanol in order to determine both singlet and triplet electronic excited states of **DCA** and **1**.

1. Gaussian 09, Revision A.1, M. J. Frisch, G. W. Trucks, H. B. Schlegel, G. E. Scuseria, M. A. Robb, J. R. Cheeseman, G. Scalmani, V. Barone, B. Mennucci, G. A. Petersson, H. Nakatsuji, M. Caricato, X. Li, H. P. Hratchian, A. F. Izmaylov, J. Bloino, G. Zheng, J. L. Sonnenberg, M. Hada, M. Ehara, K. Toyota, R. Fukuda, J. Hasegawa, M. Ishida, T. Nakajima, Y. Honda, O. Kitao, H. Nakai, T. Vreven, J. A. Montgomery, Jr., J. E. Peralta, F. Ogliaro, M. Bearpark, J. J. Heyd, E. Brothers, K. N. Kudin, V. N. Staroverov, R. Kobayashi, J. Normand, K. Raghavachari, A. Rendell, J. C. Burant, S. S. Iyengar, J. Tomasi, M. Cossi, N. Rega, J. M. Millam, M. Klene, J. E. Knox, J. B. Cross, V. Bakken, C. Adamo, J. Jaramillo, R. Gomperts, R. E. Stratmann, O. Yazyev, A. J. Austin, R. Cammi, C. Pomelli, J. W. Ochterski, R. L. Martin, K. Morokuma, V. G. Zakrzewski, G. A. Voth, P. Salvador, J. J. Dannenberg, S. Dapprich, A. D. Daniels, Ö. Farkas, J. B. Foresman, J. V. Ortiz, J. Cioslowski, and D. J. Fox, Gaussian, Inc., Wallingford CT, 2009.

2. G. Scalmani and M. J. Frisch, J. Chem. Phys., 2010, 132, 114110-114125.

Section SI 3

Singlet oxygen analysis by near-IR phosphorescence detection.

Under continuous irradiation of a sensitizer (PS), the quantum yield of $^1O_2$ emission is given by:

$$\Phi_e = C\, S_e / P_a^{PS} \quad \text{(SI 1)}$$

where C is a proportionality factor depending on geometric and electronic characteristics of the detection system and on specific parameters of the medium (refractive index, NIR absorbance), S_e is the $^1O_2$ signal intensity, P_a^{PS} (einstein L^{-1} s^{-1}) is the photon flux absorbed by the sensitizer at the wavelength of excitation.

According to the Beer-Lambert law, P_a depends on the absorbance of the PS at the excitation wavelength (A_{PS}):

$$P_a^{PS} = P_0\,(1\text{-}10^{-A_{PS}}) = P_0\ \alpha_{PS} \quad \text{(SI 2)}$$

where P_0 (einstein L^{-1} s^{-1}) is the incident photon flux and α_{PS} the absorption factor of the PS, at the wavelength of excitation.

Φ_e may be also expressed as:

$$\Phi_e = \Phi_\Delta^{PS}\, k_e\, \tau_\Delta \quad \text{(SI 3)}$$

where k_e (s^{-1}) is the rate constant of $^1O_2$ emission and τ_Δ (s) the $^1O_2$ lifetime in the system considered. In the absence of a quencher,

$$\tau_\Delta = 1/k_d \quad \text{(SI 4)}$$

where k_d (s^{-1}) is the rate constant of $^1O_2$ deactivation by the solvent ($k_e << k_d$ in most solvents).[3-5]

In the presence of a quencher that may be the photosensitizer itself (Q = PS),

$$\tau_\Delta^Q = \frac{1}{(k_d + k_t^Q[Q])} \quad \text{(SI 5)}$$

where k_t^Q (M^{-1} s^{-1}) is the rate constant of $^1O_2$ total quenching (sum of physical and chemical quenching, $k_t^Q = k_r + k_q$) by Q. k_t^{PS} and Φ_Δ^{PS} may be determined by relative measurements, using a reference sensitizer (R) of known quantum yield of singlet oxygen production (Φ_Δ^R). Combining eqns. SI 1 to SI 5, the ratio of the $^1O_2$ luminescence quantum yields for PS and R in the same solvent is given by:

$$\frac{\Phi_e^{PS}}{\Phi_e^R} = \frac{\Phi_\Delta^{PS}}{\Phi_\Delta^R}\,\frac{k_d + k_t^R[R]}{k_d + k_t^{PS}[PS]} = \frac{C_{PS}\, S_e^{PS}}{C_R\, S_e^R}\,\frac{P_0^R\, \alpha^R}{P_0^{PS}\, \alpha^{PS}} \quad \text{(SI 6)}$$

This expression simplifies to eq. SI 7 when the following conditions are satisfied:

- the absorbance of the sample and the reference are the same at the corresponding wavelengths of excitation: in this case, the absorption factors (α) and the apparatus factors (C) are identical in both cases. Corrections for small differences in absorption factors may be introduced (eq. SI

7),

- $k_t^{\mathrm{R}}[\mathrm{R}] \ll k_d$ in the range of concentration considered,
- the PS under analysis and the reference are excited at the same wavelength ($P_0^{\mathrm{R}}/P_0^{\mathrm{PS}}$ = 1).

$$\frac{S_e^R\ \alpha^{\mathrm{PS}}}{S_e^{\mathrm{PS}}\ \alpha^{\mathrm{R}}} = \frac{\Phi_\Delta^{\mathrm{R}}}{\Phi_\Delta^{\mathrm{PS}}}\ (1 + \tau_\Delta k_t^{\mathrm{PS}}[\mathrm{PS}]) \qquad \text{(SI 7)}$$

Under these conditions, the plot of $(S_e^{\mathrm{R}}/S_e^{\mathrm{PS}})(\alpha^{\mathrm{PS}}/\alpha^{\mathrm{R}}) = f([\mathrm{PS}])$ should be linear and values of k_t^{PS} and $\Phi_\Delta^{\mathrm{R}}/\Phi_\Delta^{\mathrm{PS}}$ may be obtained from the slope and the intercept of this plot if the value of τ_Δ in the solvent used is known.

An apparent value of $\Phi_\Delta^{\mathrm{PS}}$ ($\Phi_{\Delta\mathrm{app}}^{\mathrm{PS}}$) at the given PS concentration may be calculated from the ratio of the $^1O_2$ signal intensities (eq. SI 8).

$$\Phi_{\Delta\mathrm{app}}^{\mathrm{PS}} = \Phi_\Delta^{\mathrm{R}} \frac{S_e^{\mathrm{PS}}\ \alpha^{\mathrm{R}}}{S_e^{\mathrm{R}}\ \alpha^{\mathrm{PS}}} = \frac{\Phi_\Delta^{\mathrm{PS}}}{(1+\tau_\Delta k_t^{\mathrm{PS}}[\mathrm{PS}])} \qquad \text{(SI 8)}$$

In the cases where $k_t^{\mathrm{PS}}[\mathrm{PS}] \ll k_d$ (negligible $^1O_2$ quenching by the PS in the range of concentrations used), the ratio $S_e^{\mathrm{R}}/S_e^{\mathrm{PS}}$ does not depend on the PS concentration and the quantum yield of $^1O_2$ production by the PS is equal to $\Phi_{\Delta\mathrm{app}}^{\mathrm{PS}}$.

3. F. Wilkinson, W. P. Helman and A. B. Ross, *J. Phys. Chem. Ref. Data*, 1995, **24**, 663.
4. R. D. Scurlock, S. Nonell, S. E. Braslavsky and P. R. Ogilby, *J. Phys. Chem.*, 1995, **99**, 3521.
5. L. A. Martinez, C. G. Martinez, B. B. Klopotek, J. Lang, A. Neuner, A. M. Braun and E. Oliveros, *J. Photochem. Photobiol. B*, 2000, **58**, 94.

Section SI 4

Singlet oxygen analysis by chemical reaction with a probe.

The rate of disappearance of a quencher (Q) by reaction with singlet oxygen is given by:

$$-\frac{d[\mathrm{Q}]}{dt} = k_r^{\mathrm{Q}}\left[{}^1\mathrm{O}_2\right][\mathrm{Q}] \qquad \text{(SI 9)}$$

where k_r^Q is the rate constant of the chemical reaction between the quencher and $^1O_2$. If singlet oxygen is produced by photosensitization under continuous irradiation, the steady-state concentration of $^1O_2$ is given by eq. SI 10:

$$\left[{}^1\mathrm{O}_2\right] = P_a^{\mathrm{PS}}\Phi_\Delta^{\mathrm{PS}}\frac{1}{k_d + k_t^{\mathrm{PS}}[\mathrm{PS}] + k_t^{\mathrm{Q}}[\mathrm{Q}]} \qquad \text{(SI 10)}$$

where $1/(k_d + k_t^{\mathrm{PS}}[\mathrm{PS}] + k_t^{\mathrm{Q}}[\mathrm{Q}])$ represents the $^1O_2$ lifetime (τ_Δ) in the presence of PS and Q, with

k_t^{PS} and k_t^{Q} (M^{-1} s^{-1}), rate constants of $^1O_2$ total quenching by the sensitizer (PS) and the quencher (Q), respectively. If there is no interference by the reaction products, it is possible to combine eqns. SI 9 and SI 10:

$$-\frac{d[Q]}{dt} = P_a^{PS}\Phi_{\Delta}^{PS}\frac{k_r^{Q}[Q]}{k_d + k_t^{PS}[PS] + k_t^{Q}[Q]} \quad \text{(SI 11)}$$

If $k_t^{PS}[PS] \ll k_d$ and $k_t^{Q}[Q] \ll k_d$, eq. SI 11 can be integrated and simplified to a first-order kinetic law:

$$\ln\left([Q]/[Q]_0\right) = -P_{a\Delta}^{PS}\Phi_{\Delta}^{PS}\left(k_r^{Q}/k_d\right) \quad \text{(SI 12)}$$

This simplification cannot be done for a [rubrene] of 5 x 10^{-5} M as the quenching by rubrene represents 35% of the quenching by the solvent. It is only possible if [rubrene] ≤ 1 x 10^{-5} M.

Section SI 5

Kinetic parameters of rubrene oxygenation by singlet oxygen.

With our analytical apparatus it was not possible to measure the rate constant of $^1O_2$ total quenching by rubrene in ACN: we thus refer to the value of (1.0 ± 0.1) × 10^8 M^{-1} s^{-1} reported by Günther *et al*..[3] We determined the rate constant of the chemical reaction between singlet oxygen and the probe (k_r) using PN as a reference sensitizer and measuring the photon flux emitted by the light source by both chemical actinometry and spectroradiometry: we obtained an average value of (9.2 ± 0.9) × 10^7 M^{-1} s^{-1}. This value is 2.4 times higher than the one reported by Günther *et al*.[6] ((3.8 ± 0.2) × 10^7 (M^{-1} s^{-1}) for rubrene in ACN. In our case it would mean that the physical quenching by rubrene is negligible ($k_t^{Q} \approx k_r$): singlet oxygen quenching by this probe is almost completely due to chemical reaction under these experimental conditions. We could not explain the significant difference between our value and the value reported by Günther *et al*.[6]

6. G. Günther, E. Lemp and A. L. Zanocco, J. Photochem. Photobiol. A: Chem., 2002, 151, 1.

Section SI 6

Actinometry. Potassium ferrioxalate, $K_3Fe(C_2O_4)_3.3H_2O$ was used as an actinometer.[7-9] 1,10-Phenantroline (Phen) was used as a complexing agent of Fe^{2+} formed during irradiation of the actinometer, and the absorbance of the complex was measured at 510 nm. A 7.4×10^{-3} M solution of potassium ferrioxalate was used, the pH being controlled with H_2SO_4. The incident photon flux P_0, defined as the total number of photons entering the solution per unit of time and unit of volume, was calculated using equation SI 13.

$$P_{0,\lambda} = \frac{n_{Fe^{2+}}}{\Phi_{Ac,\lambda} t} \qquad \text{SI 13}$$

where

$$n_{Fe^{2+}} = \frac{N_a \alpha \Delta A_{510}}{10^3 l \varepsilon_{510}} \qquad \text{SI 14}$$

where N_A is Avogadro's number, α a dilution correction factor, ΔA_{510} the variation of the absorbance at 510 nm due to the formation of a complex between Phen and the formed Fe^{2+} ions, l the optical path length of the spectrophotometric cell, ε_{510} the molar absorption coefficient of the complex, $n_{Fe^{2+}}$ the number of Fe^{2+} ions formed upon irradiation, $\Phi_{Ac,\lambda}$ the quantum yield of the production of Fe^{2+} from potassium ferrioxalate, t the irradiation time. Solutions of ferrioxalate have been irradiated at 385 nm for variable irradiation times; from the absorbances at 510 nm and the value of $\Phi_{Ac,\lambda}$ (1.13 at 385 nm), the value of P_0 was calculated. We obtained a mean value of $(3.3 \pm 0.4) \times 10^{14}$ photons s^{-1} (i.e. $(1.8 \pm 0.5) \times 10^{-7}$ einstein L^{-1} s^{-1}) for the incident photon flux.

To check the value obtained by actinometry, we measured by spectroradiometry the radiant exitance of the light source at the selected wavelength of 385 nm. We measured a total irradiance of 9.9×10^{-5} W cm^{-2}, for a corresponding value of the photon irradiance of $(1.92 \pm 0.4) \times 10^{14}$ photons cm^{-2} s^{-1}. This value is in good agreement with the photon irradiance ($(1.98 \pm 0.4) \times 10^{14}$ photons cm^{-2} s^{-1}) calculated from the photon flux obtained by actinometry (vide supra), taking into account the irradiated surface on the spectrophotometric cell and the volume of solution used.

7. H. J. Kuhn, S. E. Braslavsky, R. Schmidt, *Pure Appl. Chem.*, 2004, **76**(12), 2105.
8. A. M. Braun, M. T. Maurette and E. Oliveros, *Photochemical technology*, Wiley-VCH, Weinheim, 1991.
9. S. E. Braslavsky *et al.*, Glossary of Terms Used in Photochemistry (3rd ed.), Pure Appl. Chem., 2007, **79**, 293-465.

Table SI 1 Molar absorption coefficients at 367, 355 and 266 nm for compounds **1**- **4** in ACN solutions at room temperature. Samples have been irradiated at 367 nm for the detection of singlet oxygen phosphorescence, and at 355 and 266 nm for the detection of the transient species by laser flash photolysis. Errors: approx. 10%

PS	ε / M^{-1} cm^{-1}		
	367 nm	**355 nm**	**266 nm**
1	8930	6470	63400
2	7340	5730	40180
3	5700	4130	37650
4	6180	4890	33320

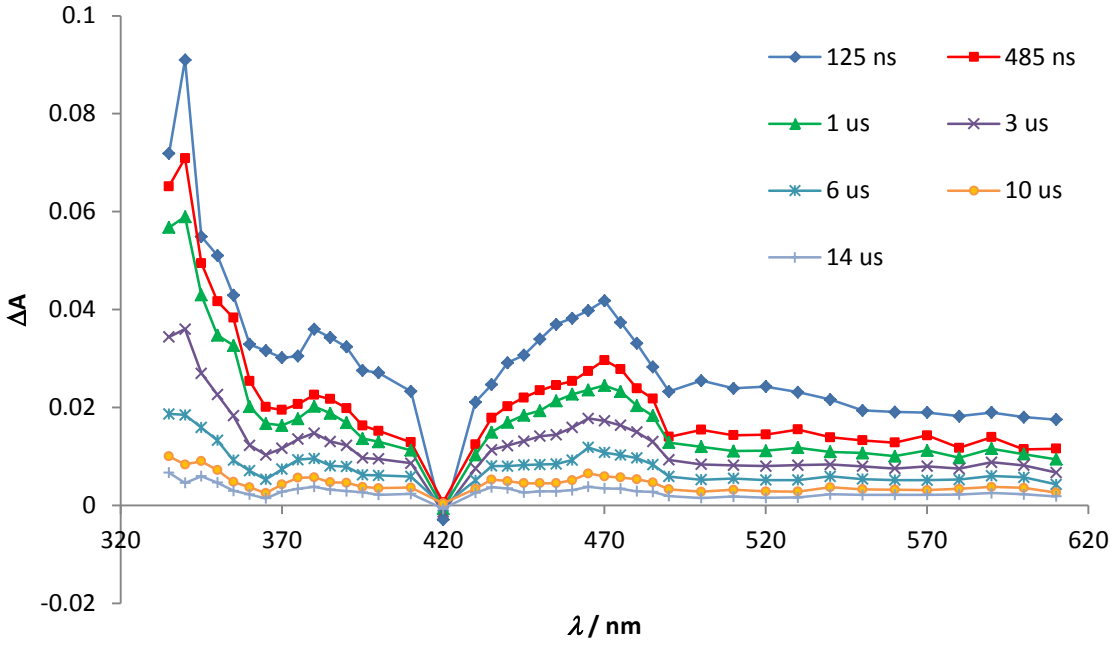

Figure SI 7 Time evolution of the transient absorption observed by laser flash photolysis of **2** at room temperature in Ar-saturated ACN solution.

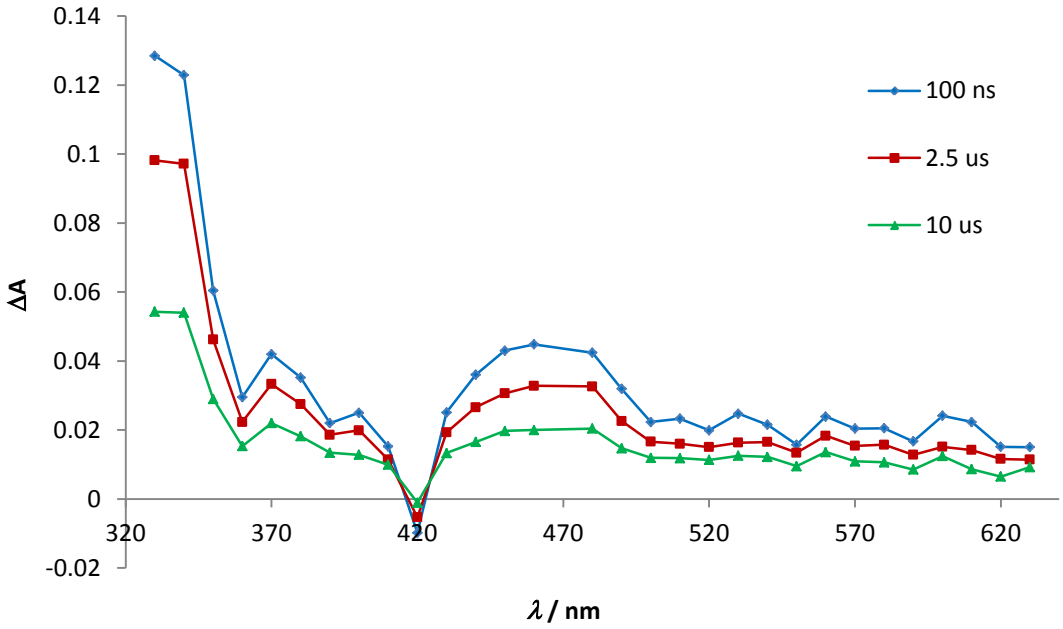

Figure SI 8 Time evolution of the transient absorption observed by laser flash photolysis of **3** at room temperature in Ar-saturated ACN solution.

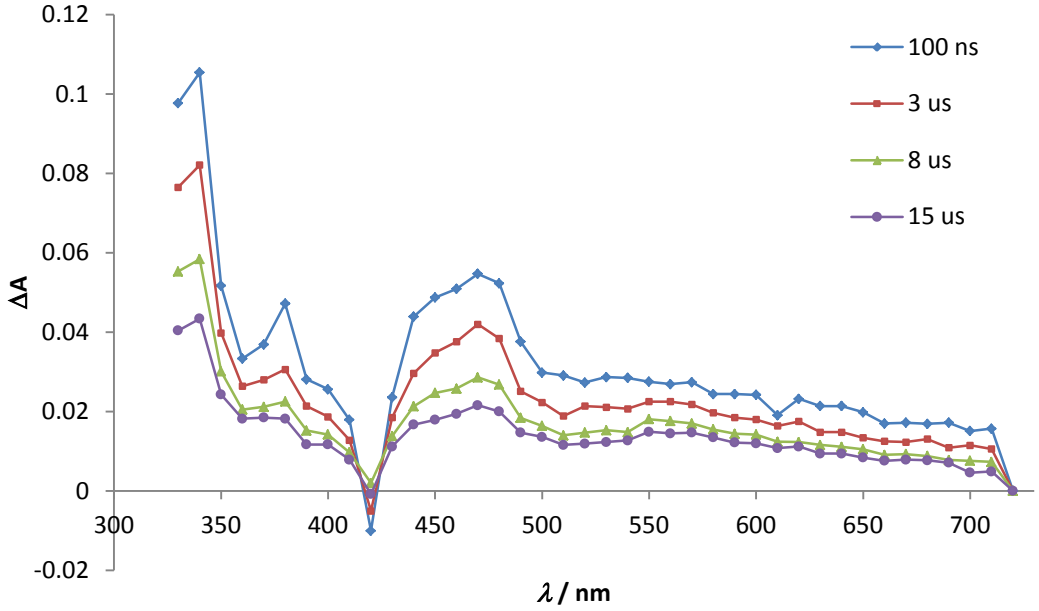

Figure SI 9 Time evolution of the transient absorption observed by laser flash photolysis of **4** at room temperature in Ar-saturated ACN solution.

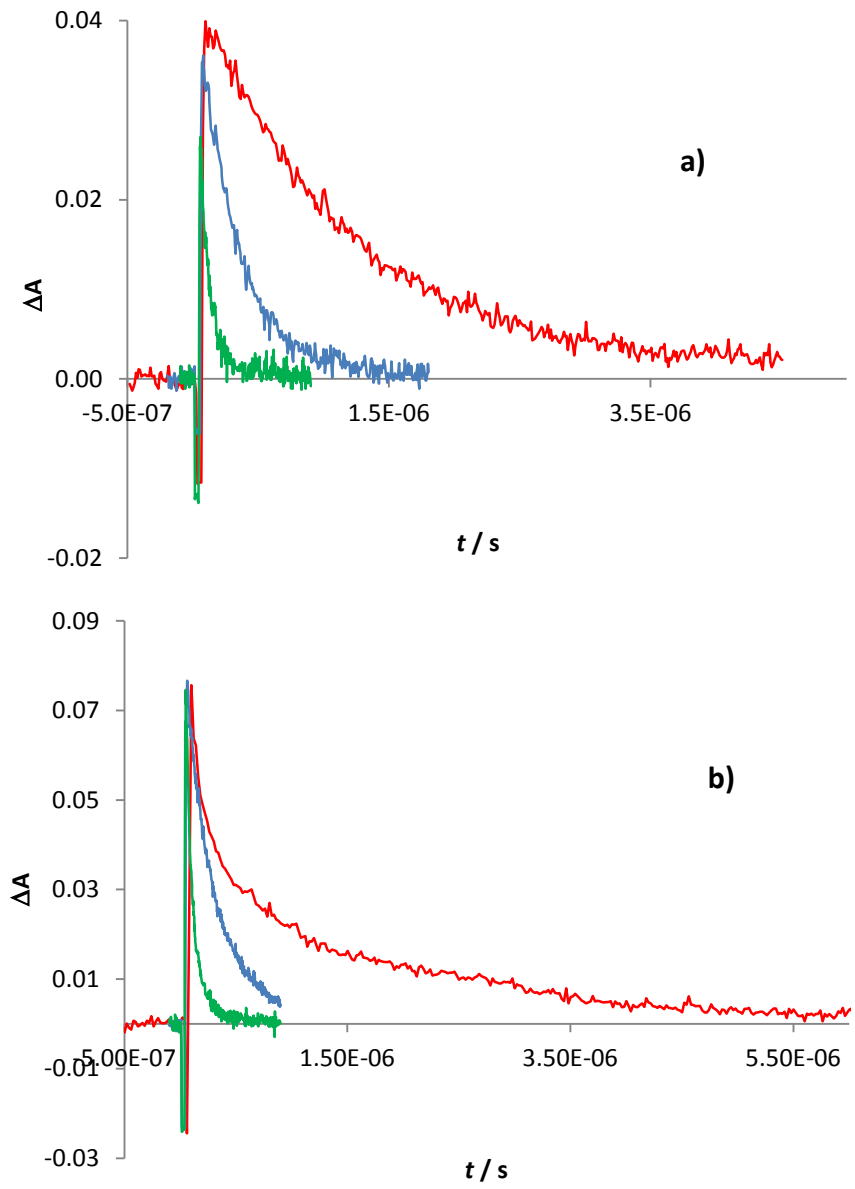

Figure SI 10 Decay of the transient absorption observed by laser flash photolysis in argon- (red line), air- (blue line) and oxygen- (green line) saturated ACN solutions at room temperature. a) **1** and b) **2**.

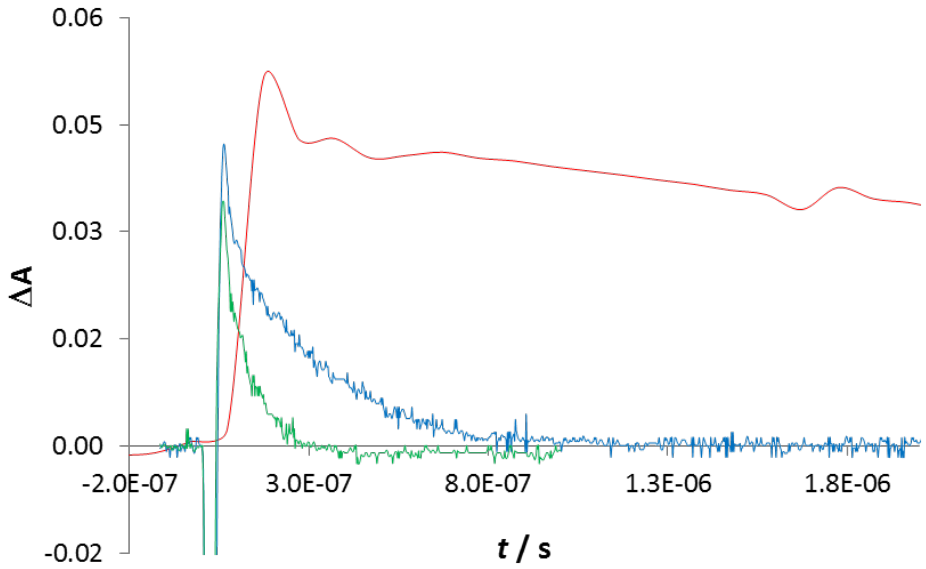

Figure SI 11 Decay of the transient absorption of **3** in argon- (red line), air- (blue line) and oxygen- (green line) saturated ACN solutions at room temperature.

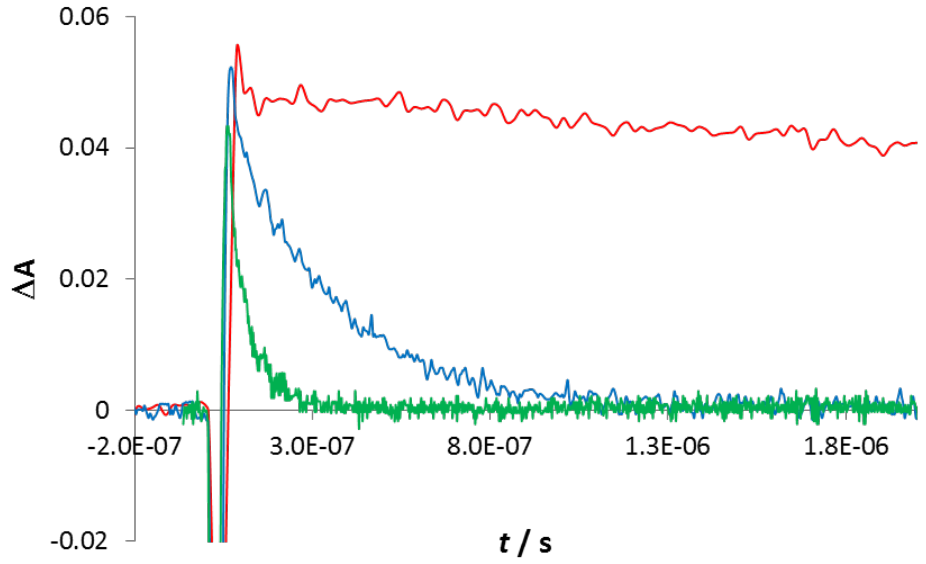

Figure SI 12 Decay of the transient absorption of **4** in argon- (red line), air- (blue line) and oxygen- (green line) saturated ACN solutions at room temperature.

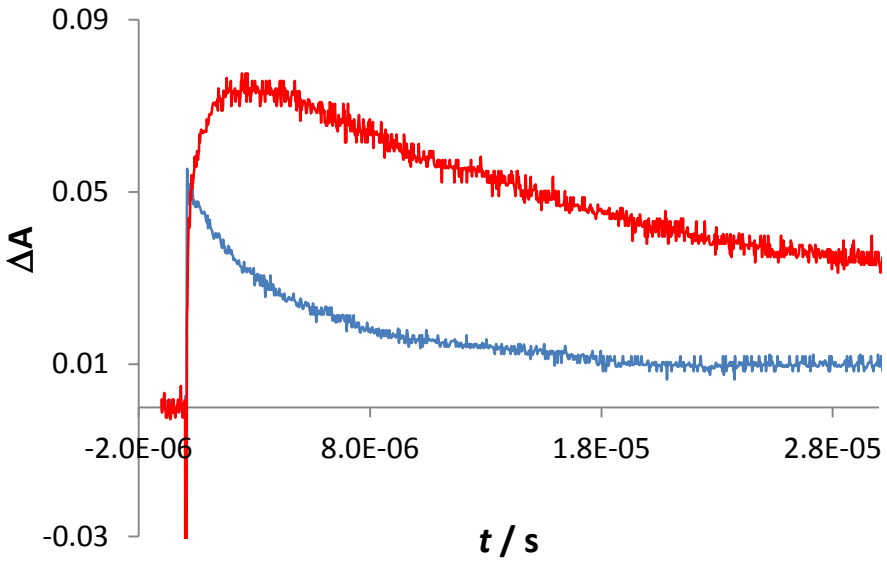

Figure SI 13 Transient absorption decay at 495 nm as a function of time in Ar-saturated ACN solutions at room temperature. Blue line: **1** (1.5×10^{-5} M); red line: **1** (1.5×10^{-5} M) and rubrene (2.0×10^{-4} M) as an energy acceptor.

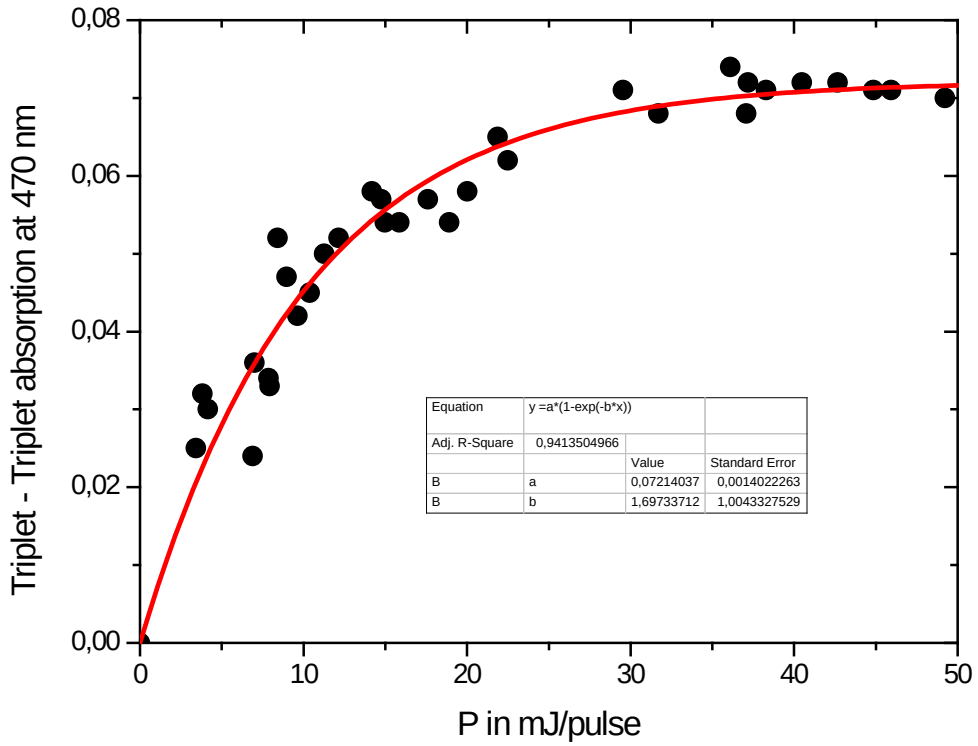

Figure SI 14 Variation of the absorbance at 470 nm upon irradiation of **1** at 266 nm in argon-saturated ACN solution as a function of the pulse energy.

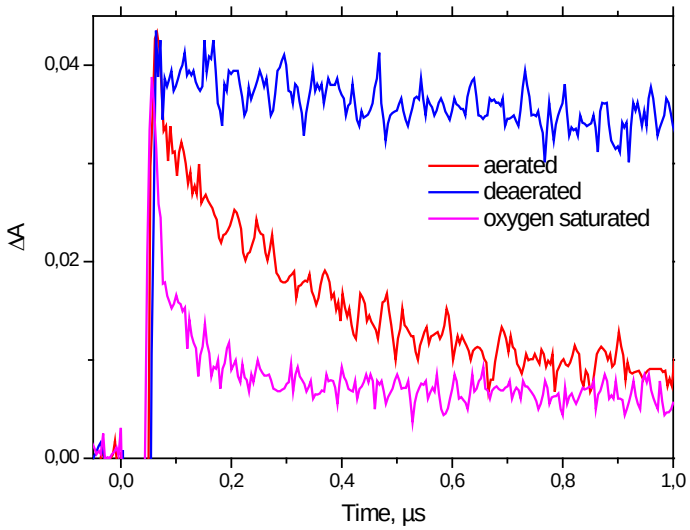

Figure SI 15 Time evolution of the transient absorption measured at 470 nm upon irradiation of **1** at 266 nm in argon-saturated ACN solution (blue line), air-saturated ACN solution (red line), oxygen-saturated ACN solution (pink line).

Table SI 2 Rate constants of transient decay (k_d^T) in argon-, air- and oxygen- saturated ACN solutions, and bimolecular rate constants of transient quenching by molecular oxygen (k_{q,O_2}^T) at room temperature for compounds from **1** to **4**.

PS	k_d^T			k_{q,O_2}^T / 10^9 M^{-1} s^{-1}
	argon / 10^5 s^{-1}	air / 10^6 s^{-1}	oxygen / 10^7 s^{-1}	
1	1.4 ± 0.2	3.4 ± 0.3	1.8 ± 0.3	2.0 ± 0.2
2	2.0 ± 0.2	3.8 ± 0.2	1.5 ± 0.5	1.7 ± 0.1
3	1.4 ± 0.2	4.0 ± 0.3	1.4 ± 0.4	1.5 ± 0.2
4	1.2 ± 0.1	3.7 ± 0.3	2.0 ± 0.4	2.3 ± 0.2

Table SI 3 Rate constants of quenching of the triplet excited state of compounds **1**-**4** by energy transfer to anthracene ($k_{q,Ant}$); quantum yields of formation of the tripled excited state of anthracene and rubrene as energy acceptors.

PS	$k_{q,Ant}$ / 10^9 M^{-1} s^{-1}	$\phi_{T,Ant}$	$\phi_{T,Ru}$
1	5.9 ± 0.6	0.17 ± 0.3	0.10 ± 0.1
2	5.5 ± 0.5	0.07 ± 0.1	0.05 ± 0.1
3	5.7 ± 0.6	0.08 ± 0.2	0.09 ± 0.1
4	-	-	0.09 ± 0.1

Table SI 4 Values of $^1O_2$ emission signals S_e^R and S_e^{PS} in ACN , at different absorbances (A^R, A^{PS}) and of $\frac{S_e^R}{S_e^{PS}}$ corrected for small differences in absorption factors α between PS (**DCA**, **1**, **2**, **3** and **4**) and reference sensitizer (R = PN); wavelength of irradiation: 367 nm.

PS	A^R (367 nm)	S_e^R / a.u.	A^{PS} (367 nm)	S_e^{PS} / a.u.	$\frac{S_e^R\,\alpha^{PS}}{S_e^{PS}\,\alpha^R}$
DCA	0.71	11.6	0.72	3.5	3.38
	0.59	10.2	0.57	3.1	3.30
	0.49	9.1	0.49	2.7	3.37
	0.37	7.9	0.38	2.3	3.46
	0.28	6.0	0.27	1.8	3.31
1	0.12	3.2	0.13	3.2	1.16
	0.17	3.6	0.20	4.1	0.97
	0.25	6.0	0.25	5.4	1.10
	0.39	7.6	0.40	7.1	1.09
	0.56	9.8	0.53	8.9	1.08
	0.63	12.2	0.63	11.0	1.11
2	0.12	3.2	0.12	2.6	1.29
	0.17	3.6	0.18	2. 5	1.42
	0.28	5.4	0.31	3.0	1.85
	0.28	5.4	0.29	3.0	1.78
	0.39	7.6	0.38	3.7	2.02
	0.56	9.8	0.55	4.2	2.33
3	0.12	3.2	0.12	2.2	1.44
	0.17	3.6	0.2	2.7	1.45
	0.25	6.1	0.25	3.5	1.69
	0.28	5.4	0.28	3.6	1.50
4	1.03	16.4	1.02	13.9	1.18
	0.81	13.6	0.81	11.1	1.18
	0.62	11.3	0.61	9.4	1.17
	0.51	9.8	0.51	8.2	1.18
	0.41	8.1	0.41	6.3	1.18

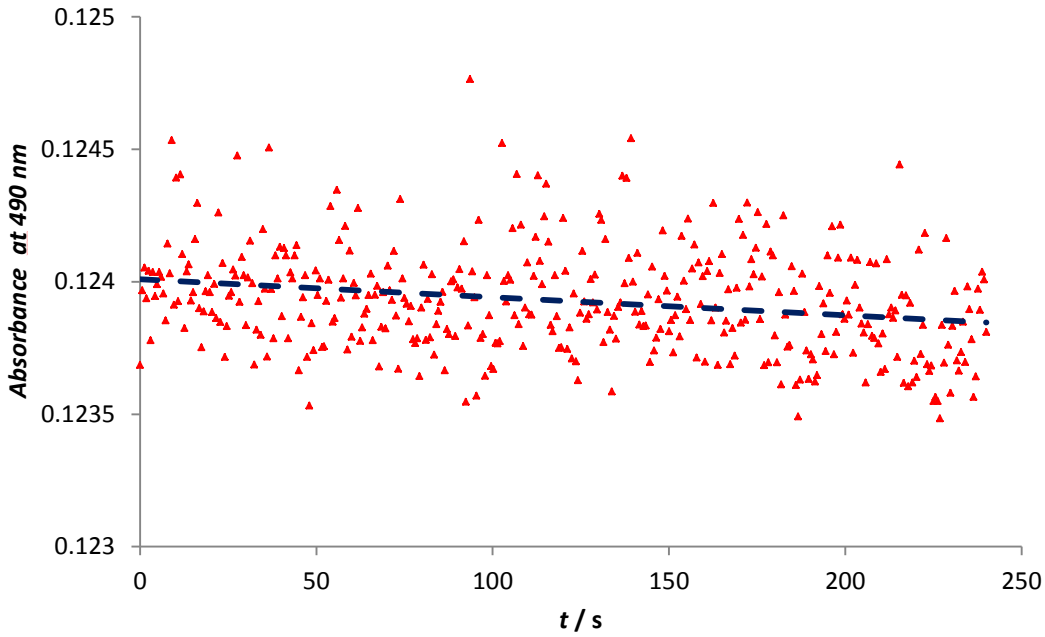

Figure SI 16 Variation of the absorption at 490 nm (maximum of absorption, red triangles) during irradiation at 385 nm (1.5×10^{-4} W cm^{-2}) of a solution containing rubrene (2.3×10^{-5} M) in the absence of photosensitizer. The absorbance was monitored during 250 s. Dashed blue line: linear fitting. Rate of rubrene consumption: 4×10^{-12} mol s^{-1}. Solvent: air-equilibrated ACN at 25 °C.

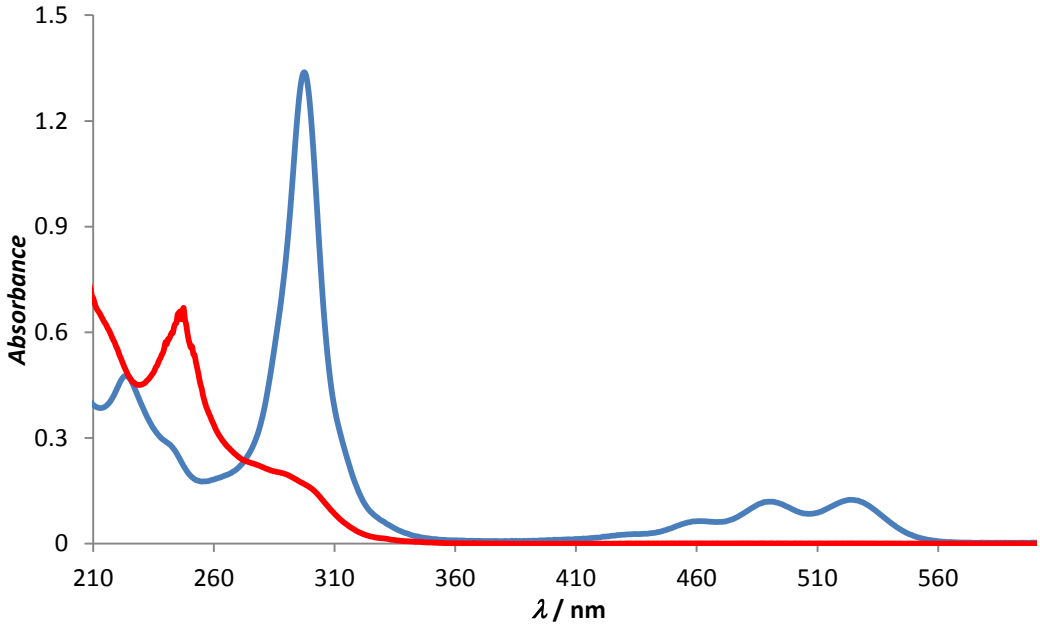

Figure SI 17 Absorption spectra of rubrene (blue) and of the endoperoxide formed by singlet oxygen addition to rubrene (red). Singlet oxygen was produced by photosensitization using PN; the spectrum of the endoperoxide was obtained after complete conversion of rubrene and the subtraction of the spectrum of the photosensitizer. Solvent: air-equilibrated ACN at 25 °C.

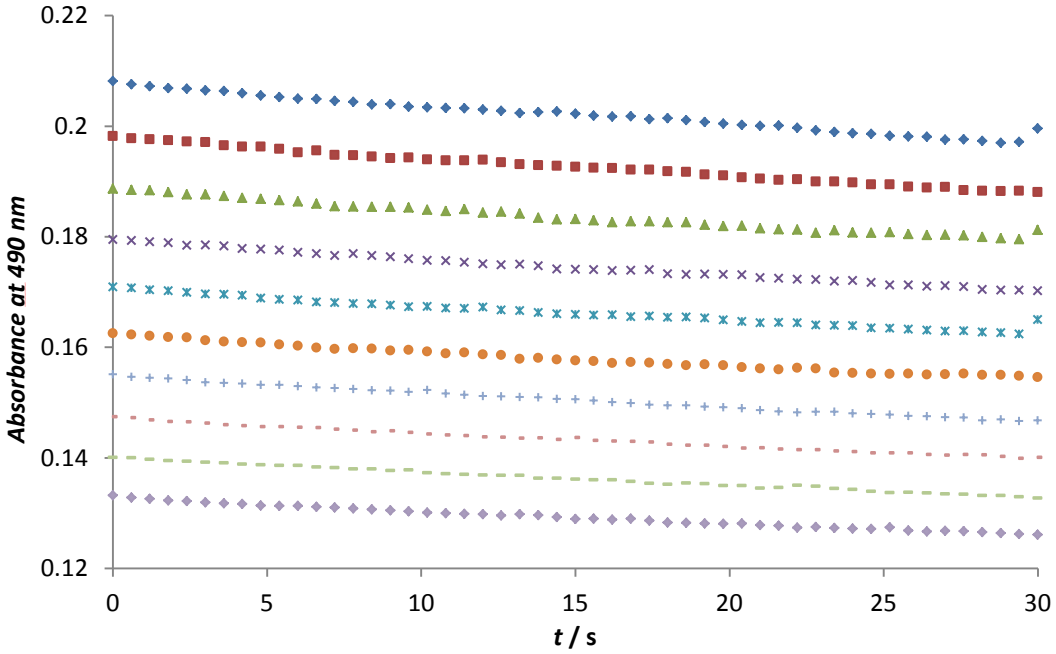

Figure SI 18 Variation of the absorbance at 490 nm (maximum of absorption of Rubrene) during irradiation of **1** (6.0×10^{-5} M) at 385 nm (1.5×10^{-4} W cm^{-2}) in air-equilibrated ACN in the presence of rubrene (4.0×10^{-5} M). The absorbance was monitored every 30 s during 5 min (each series corresponding to subsequent 30 seconds irradiation times). Rate of rubrene consumption: 2×10^{-10} mol s^{-1}. Temperature: 25 °C.

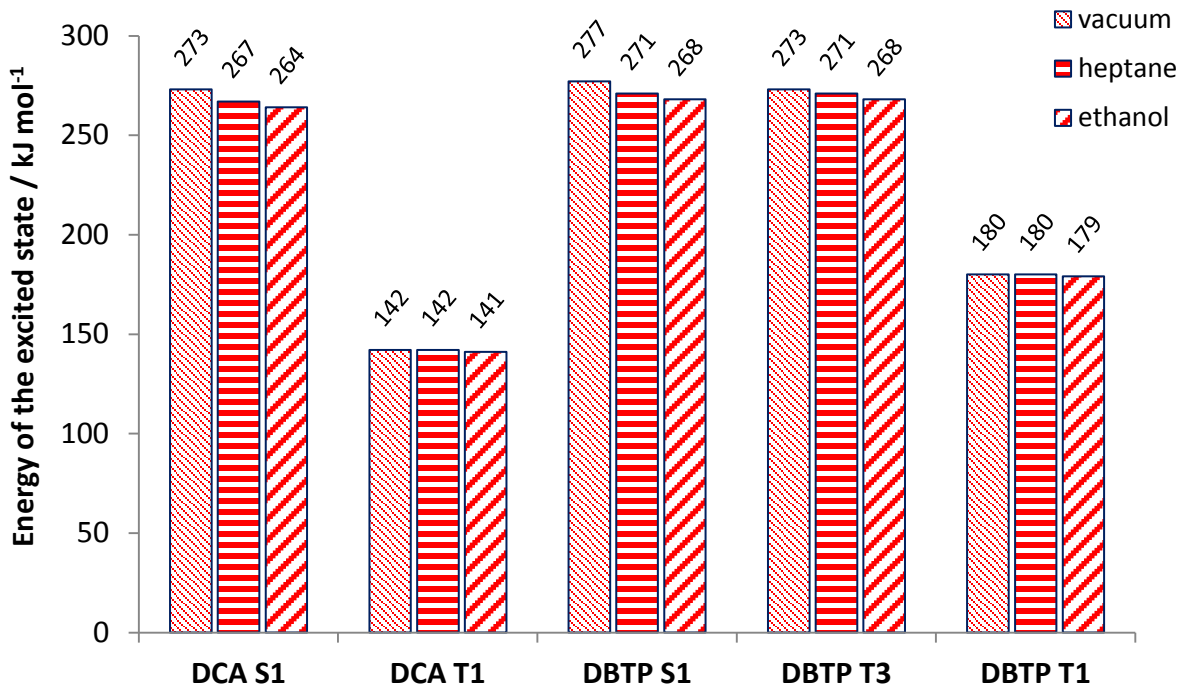

Figure SI 19 Energy levels of DCA S_1 and T_1 states and of DBTP S_1, T_3 and T_1 states, calculated for vacuum, heptane and ethanol.